Argo floats revealing bimodality of large-scale mid-depth circulation in the North Atlantic

CHU Peter C[1], LVANOV Leonid M[1], MELNICHENKO Oleg V[2], and Li Rongfeng[3]

1. Department of Oceanography, Naval Postgraduate School, Monterey, California, USA

2. International Pacific Research Center, University of Hawaii at Manoa, Hawaii, USA

3. Institute of Atmospheric Physics, Chinese Academy of Sciences, Beijing 100029, China

Abstract

Analysis of Argo float trajectories at 1000 m and temperature at 950 m in the North Atlantic between November 2003 and January 2005 demonstrates the existence of two different circulation modes with fast transition between them. Each mode has a pair of cyclonic – anticyclonic gyres. The difference is the location of the cyclonic gyre. The cyclonic gyre stretches from southeast to northwest in the first mode and from the southwest to the northeast in the second mode. The observed modes strongly affect the heat and salt transport in the North Atlantic. In particular, the second mode slows down the westward transport of the warm and saline water from the Mediterranean Sea.

Key words：

1   Introduction

Although the North Atlantic is a subject of intensive theoretical and observational studies for many years, knowledge on the large – scale mid – depth circulation and especially on its variability is quite limited. There are several attempts to construct the large – scale mid – depth circulation pattern for the whole North Atlantic using climate data (Schmitz and McCartney, 1993; Reid, 1994; Lozier et al., 1995) and for regional seas in the North Atlantic with higher resolution using subsurface float (SO-FAR, RAFOS, ALACE, PALACE, SOLO) trajectories directly or combining with hydrological obser-

vations (Lavender et al., 2000; Lavender et al., 2005; Zhang et al., 2001; Bower et al., 2002). The-basin scale and subbasin-scale mid-depth circulation and its variability can also be potentially extracted from the Argo float data (Argo Science Team, 2001). However, analysis of Argo data is not a trivial problem because the observation is sparse (up to 800 km spatial gap) and noisy.

2   Data and quality control

Between November 2003 and January 2005, over 56 000 float days (cumulative) of data were collected in the North Atlantic (10° ~60°N) in general at three parking depths：1 000, 1 500 and

2 000 m. The floats parking at 2 000 m, depths shallower than 1 000 m, and unknown depths are excluded from the analysis. Temperature at 950 m and trajectories at 1 000 and 1 500 m are extracted from all the existing Argo floats. The data from 1 000 and 1 500 m were grouped together to represent the mid-depth.

The measurement cycle of an Argo profiling float includes four stages: ascending, surface drifting, diving and deep drifting. The Argo float can only get its position fixings while it ascends to the sea surface. The vector between two consecutive surface positions during the deep drifting divided by the time interval is taken as the mid-depth velocity vector. When the Argo float is diving, ascending and drifting below the sea surface, no data can be transmitted to the ground stations in real time. Velocity field after the first step analysis shows noisy circulation patterns (Figs 1a, and b) with large spatial gaps (from 230 to 800 km).

Uncertainty in the Argo float data causes errors in the velocity field. First, the data extracted from the floats parking at two different levels: 1 000 and 1 500 m and grouped together to represent the mid-depth (1000 m). This neglects the vertical shear. Second, the vertical shear causes increase or decrease of the distance between the points of ascending from and diving to the parking depth. Thirdly, the sequence of float trajectory segments only approximates the real Lagrangian paths. Fourthly, preliminary computations (not included here to be published in a separate paper) show that high resolution elements of circulation in the western North Atlantic, such as the northern recirculation gyre and the Deep Western Boundary Current (DWBC) are also revealed by the Argo floats. For example, Figs 1a and b clearly show the existence of DWBC. However, such a resolution is not available for the whole North Atlantic. The high-energetic mesoscale eddies and narrow boundary currents are classified as "noise" and removed from the analysis. Fifthly, there are large spatial gaps in Argo float trajectories.
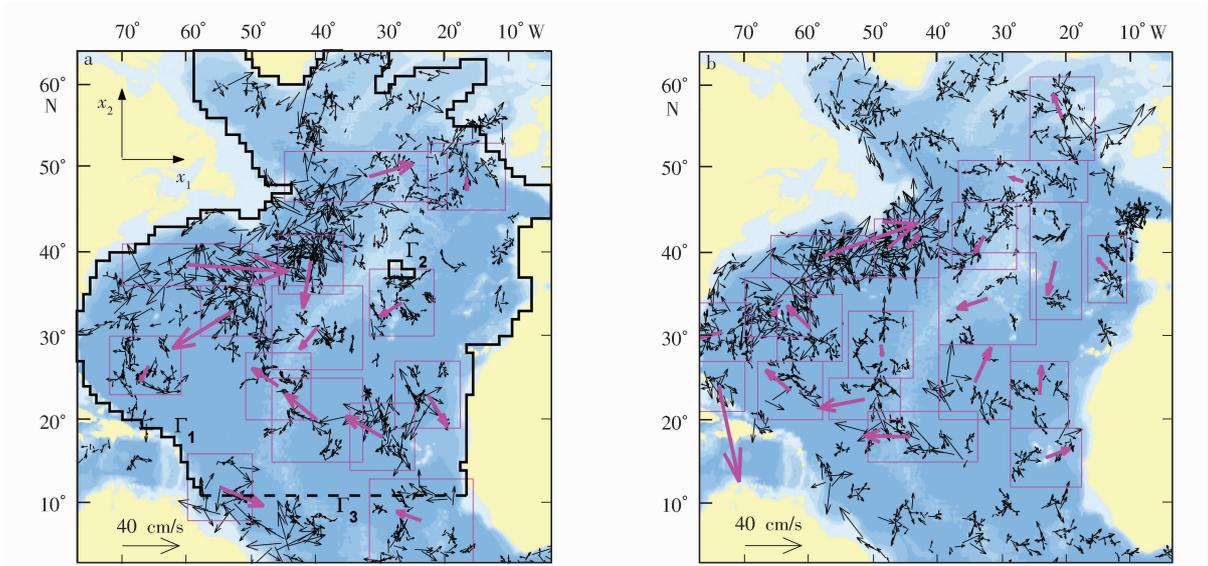

Fig. 1.   Circulation velocities (tiny arrows) estimated from the original Argo float tracks at 1000 m for December 2003—Mar 2004 (a) and August 2004—November 2004 (b). The figure scale is given for tiny arrows. Red arrows are circulation velocities obtained by averaged over appropriate bins (red lines). The magnitudes of these arrows are multiplied by the scale equaled 20 for better visualization of schematic circulation patterns. Γ_1, Γ_2 and Γ_3 are boundaries of the computation area.

The temperature observation has higher quality than the velocity observation since the former has (1) higher resolution and (2) less spatial gaps. Figure 2 shows typical monthly coverage of observations. Interested readers can find the detailed discussion on the navigation errors and measurement errors caused by temperature sensors in http://argo. jcommops. org.
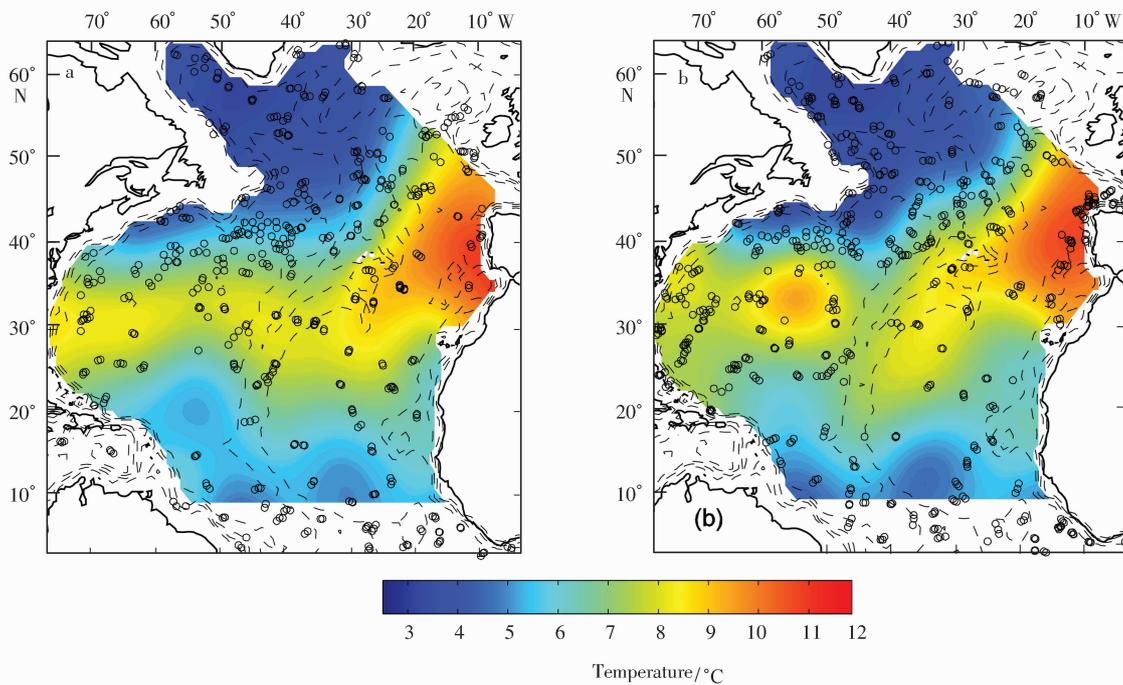

Fig. 2.   Monthly temperature at 950 m for Feburary 2004 (a) and December 2004 (b). Circles are points where temperature was measured. The zero flux boundary condition is used at Γ_1, Γ_2 and Γ_3 to reconstruct temperature patterns (see, explanation in Chu et al. , 2003a).

Three quality control steps are performed to identify and remove temperature profiles corrupted by large measurement errors. (1) Explicitly absurd profiles were removed after a visual inspection. (2) A portion of temperature profiles, which were outside of the prescribed accuracy of the climatic data (Levitus et al. , 1998), were also excluded from the further analysis. (3) Temperature snapshots computed by the optimal spectral decomposition (OSD) method (Chu et al. 2003a, 2004) should not show explicit outbreaks in temperature structure. Any temperature profile contributing to such outbreaks was a subject to removing.

A parking depth for each Argo float was extracted from a "meta" file as the variable "PARKING_ PRESSURE" (http://www. Argo. ucsd. edu). To control the parking depth the variable "PRES" (a pressure measured along the float trajectory) from a file containing float trajectory data, was used. Most floats launched in the area of interest have measured this variable.

3   Methodology

Two-step analysis is used in this study. First, the bin technology (Davis, 1991) is used to get the first-guess mid-depth velocity (temperature) field from the Argo float trajectories (temperature) at

1000 m (950 m) (see Figs 1a and b). Second, the optimal spectral decomposition (OSD) method (Eremeev et al. , 1992; Ivanov et al. , 2001; Chu et al. , 2003a, b, 2004; Chu et al. , 2007) is used to reconstruct circulation and temperature patterns from the first-guess fields with higher resolution.

Any field (temperature, salinity, or velocity) can be decomposed into generalized Fourier series using the OSD method. The three-dimensional field is then represented by linear combination of the products of basis functions (or called modes) and corresponding Fourier coefficients at point x of the interested area (Ω),

$$T(x,t) = T_0 + \sum_{l=1}^{L} D_l(t) \Xi_l(x,t), \quad (1)$$

where $\{\Xi_1\}$ is the basis functions; $\{D_l(t)\}$ is the spectral coefficients; and T_0 is the mean temperature over the interested area (Ivanov et. al. , 2001; Chu et al. , 2004). The least square method is used to determine the spectral coefficient and the mean temperalure (Thiebaux and Pedder, 1987).

If a rectangular closed ocean basin is considered, the basis functions are sinusoidal functions. If a realistic ocean basin is considered, the basis functions are the eigenvalues of the three – dimensional Laplace operator with real topography. One major benefit of using the OSD method is that the boundary conditions for the ocean variables (temperature, salinity, velocity) are always satisfied.

After the decomposition, the three – dimensional field is represented by a set of Fourier coefficients. This method has three components: (1) determination of the basis functions; (2) optimal mode truncation; and (3) determination of the Fourier coefficients. Determination of basis functions is to solve the eigenvalue problem. Chu et al. (2003a, b) developed a theory to obtain the basis functions with open boundaries. The basis functions are only dependent on the geometry of the ocean basin, not dependent on the oceanic variables. This is to say,

no matter which variable (temperature, salinity, or velocity) is concerned, the basis functions are the same, and can be predetermined before the data analysis. For data without error, the more the modes, the more the accuracy of the processed field. For data with error, this rule of the thumb is no longer true. Inclusion of high – order modes leads to increasing error. The Vapnik variational principal (Vapnik, 1982) is used to determine the optimal mode truncation. After the mode truncation, optimal field estimation is to solve a set of a linear algebraic equation of the Fourier coefficients. This algebraic equation is usually ill – posed. The rotation method (Chu et al. , 2004) is developed to change the matrix of the algebraic equation from ill – posed to well – posed such that a realistic set of the Fourier coefficients are obtained.

Thus, the OSD method has two major features. First, a special constraint (Vapnik, 1982) is used to determine the optimal truncation for to compromise between spectral representation and ability to fit the observations. For number of basis functions more than the optimal truncation, the model contains too much contributions from noise. For number of basis functions less than the optimal truncation, the model resolution is too coarse to fit the observations.

The optimal truncation determines the real spatial resolution of the reconstructed field and depends on the noise level and degree of inhomogeneity of observation coverage. It fills large spatial gaps in observation coverage. Interested readers are referred to Chu et al. (2003a, b, 2004; Chu et al. , 2007) where all the technical details and features of the OSD method are explained. After the spectral coefficients and mean teroperature are determined from the observational data $T(x_p)$, the temperature field with regular temporal – spatial grids is obtained using Eq. (1).

A vector field (such as velocity) at the point x of the interested area is represented by

$$\vec{U}(x) = C\nabla \Psi_0(x) + \sum_{n=1}^{N} A_n \nabla \times [\vec{k}\Psi_n(x)] +$$
$$\sum_{m=1}^{M} B_m \nabla \cdot \Phi_m(x), \qquad (2)$$

where $\Psi_n(x)$ and $\Phi_m(x)$ are the basis functions; A_n and B_m are the spectral coefficients; $\vec{k}$ is the unit vector in the vertical (upward positive) direction; ∇ is the horizontal gradient operator; $\Psi_0(x)$ and C are the harmonic function and its coefficient for the multiconnected area of the interested area with three boundaries Γ_1, Γ_2, Γ_3 (Fig. 1a). All other notations are the same as for temperature. The optimal mode truncations M_{opt} and N_{opt} are determined using Vapnik's (1982) technology. After the basis functions $[\Psi_n(x), \Phi_m(x) | n = 1, \cdots, N_{opt}; m = 1, \cdots, M_{opt}]$ the harmonil function and its coefficient and $[\Psi_0(x), C]$ are determined from the observational data $\vec{U}(x)_p = [U_1(x_p), U_2(x_p)]$ collected within some time period, the velocity vector field with regular temporal – spatial grids is obtained using Eq. (2).

Comparison among OSD, optimal interpolation, and smoothing – spline (Chu et al., 2003a, b) shows great advantage of the OSD method in filling large gaps (spatial and temporal) in observational coverage and removing noises with various scales effectively from the data. These features are the key to select the OSD method for the analysis of the Argo data.

4   Estimation of positioning errors

As we mentioned previously, no data can be transmitted to the ground stations in real time below the sea surface. However, the vertical geostrophic shear may be strong especially in the west boundary current. Therefore, estimation of positioning errors is needed in calculating the intermediate – depth velocity from Argo trajectory data. Park et al. (2005) have assumed that a surface Argo float trajectory consists of large – scale drift, inertial motion, and

measurement noise. For temporal scales longer than two months, the inertial motions may be considered as spatially uncorrelated "noise" and effectively removed by the OSD.

Systematic float shifts caused by large – scale currents in upper ocean layer are estimated following Chu et al. (2007). A location of the pth float $\hat{x}_p$ at the parking depth H_p^0 is specified by deduction of the "effective" displacement from a location of the same float x_p after ascending or before descending to the parking depth:

$$\hat{x}_p = x_p - \int_{t_p}^{t'_p} U(wt)\,dt \qquad (3)$$

where $\delta t = t_p - t'_p$, is the ascending/descending time; w and is a velocity of ascending or descending. A phenomenological model is used for U_p:

$$U_p = \begin{cases} U_p^{sf} \exp(-\sigma_p z), & z \leqslant \hat{H}_p, \\ \hat{U}_p, & z > \hat{H}_p, \end{cases} \qquad (4)$$

where U_p^{sf} and $\hat{U}_p$ are the surface and mid-depth velocities estimated from the surface and subsurface tracks of the pth float, respectively; $\hat{H}$ is the low boundary of the oceanic thermohaline estimated from temperature profile of the same float; $\sigma_p = -1/(2\hat{H}_p) \log (\hat{U}^2/\bar{U}^2)$. For Argo floats launched in the area of interest we have

$$U^{sf} \approx 15 - 20 \text{ cm/s}, \ \hat{U} \approx 5 - 10 \text{ cm/s},$$
$$\hat{H} \approx 300 \text{ m}, \ \delta t = 10 \text{ h}. \qquad (5)$$

Substituting values of Eq. (5) into Eqs. (3) and (4) yields that on an average the position error for the Argo float launched in the area of interest should be less than 6 km. That results in the systematic drift for floats less than 0.6 cm/s. Therefore, although the position error of each float was corrected by the method described above, the upper ocean drifting effects does not contribute too much into the reconstruction error.

5   Results

The two different circulation modes (Figs 1 a

and b) are barely recognized from the Argo float velocity using the bin technology. The arrows are the mean velocities averaged over appropriate bines shown in the same figures. The circulation patterns, robust to variations of bin sizes, show well – known circulation features identified from early analyses on the RAFOS float trajectories in separate regions of the North Atlantic. For example, across the Mid-Atlantic Ridge transport of cooler and fresher Labrador Sea water at about 50° N (Paillet et al., 1998) is clearly seen in Fig. 1a. Note that the bin technology is unable to remove stochastic noises from the observations. Davis (1991) also pointed out numerical biases of this technology. Therefore, the results from the bin technology (Figs 1 a and b) are crude assessments of the reality.

Different temperature patterns should correspond to these circulation modes since they are very distinct features. To confirm this, we reconstructed 14 monthly temperature fields between December 2003 and January 2005 with the optimal truncation of 38, temperalure of 6.50 ℃ and the basis function on 1° × 1° grid. These computations uniquely demonstrate the existence of two different temperature patterns for February 2004 (Fig. 2a) and December 2004 (Fig. 2b).

The principle distinction between these patterns appears at least in cross-Atlantic transport of heat from the Mediterranean Sea. The first mode implies the existence of advection pathways across the Mid – Atlantic Ridge, which may accelerate westward motion of the Mediterranean water in the North Atlantic. The second mode slows down westward propagation of warm and salt water from the Mediterranean Sea. Comparison of monthly temperature patterns consecutively from September to December 2004 (the second mode period, not shown here) clearly demonstrates a largest portion of Mediterranean water slowly moves along the Mid-Atlantic Ridge at speed of about 1.0 ~ 1.5 cm/s. If the mid-depth temperature is taken as a tracer, the velocity can be roughly estimated from two consecutive temperature fields on the base of displacements of 6, 7, 8, 9 and 10 ℃ isotherms (Figs 3 a and b) where the arrows show the mean direction of isotherm displacements during three month periods.
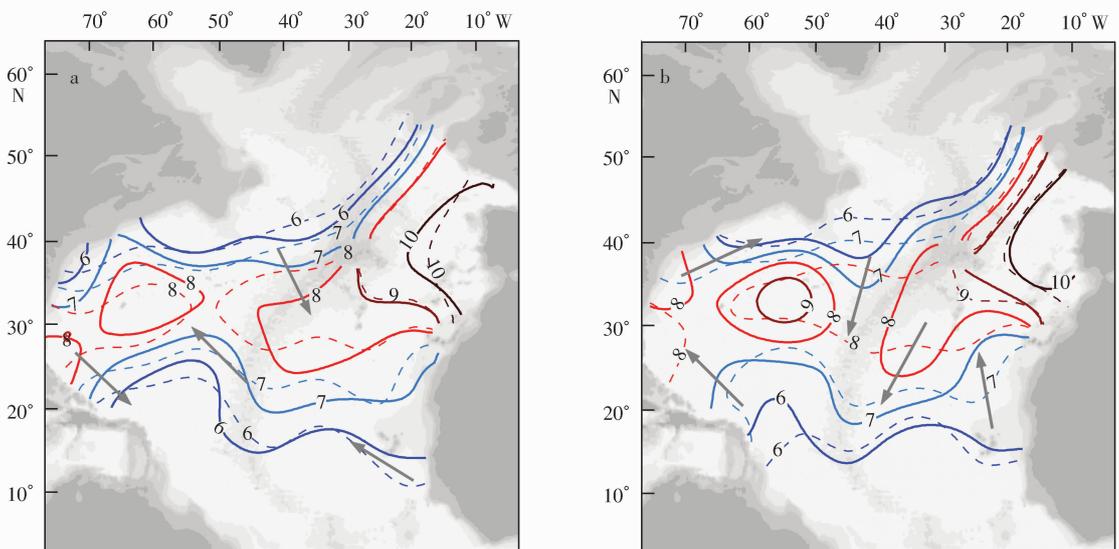

Fig. 3.   The cartoons of mid-depth circulation drawn from the analysis of isotherm displacements for December 2003—March 2003 (a) and September 2004—December 2004 (b). Dashed and solid lines are monthly isotherms for December 2003— March 2004 in a and for September 2004—December 2004 in b. The gray arrows schematically show water pathways.

Spatial distributions of both modes are reconstructed for $N_{opt} = 24$, $M_{op} = 3$, $C = 3.2 \times 10^7$ and the basis functions calculated on $1° \times 1°$ grid. Two distinct circulation modes and a transition between them are identified from these computations (Figs 4 a, b and c). The first mode represents a pair of cyclonic – anticyclonic gyres and two gyres of smaller size in the Labrador Sea and the eastern North Atlantic (Fig. 4a). This mode dominates from December 2003 to March 2004.
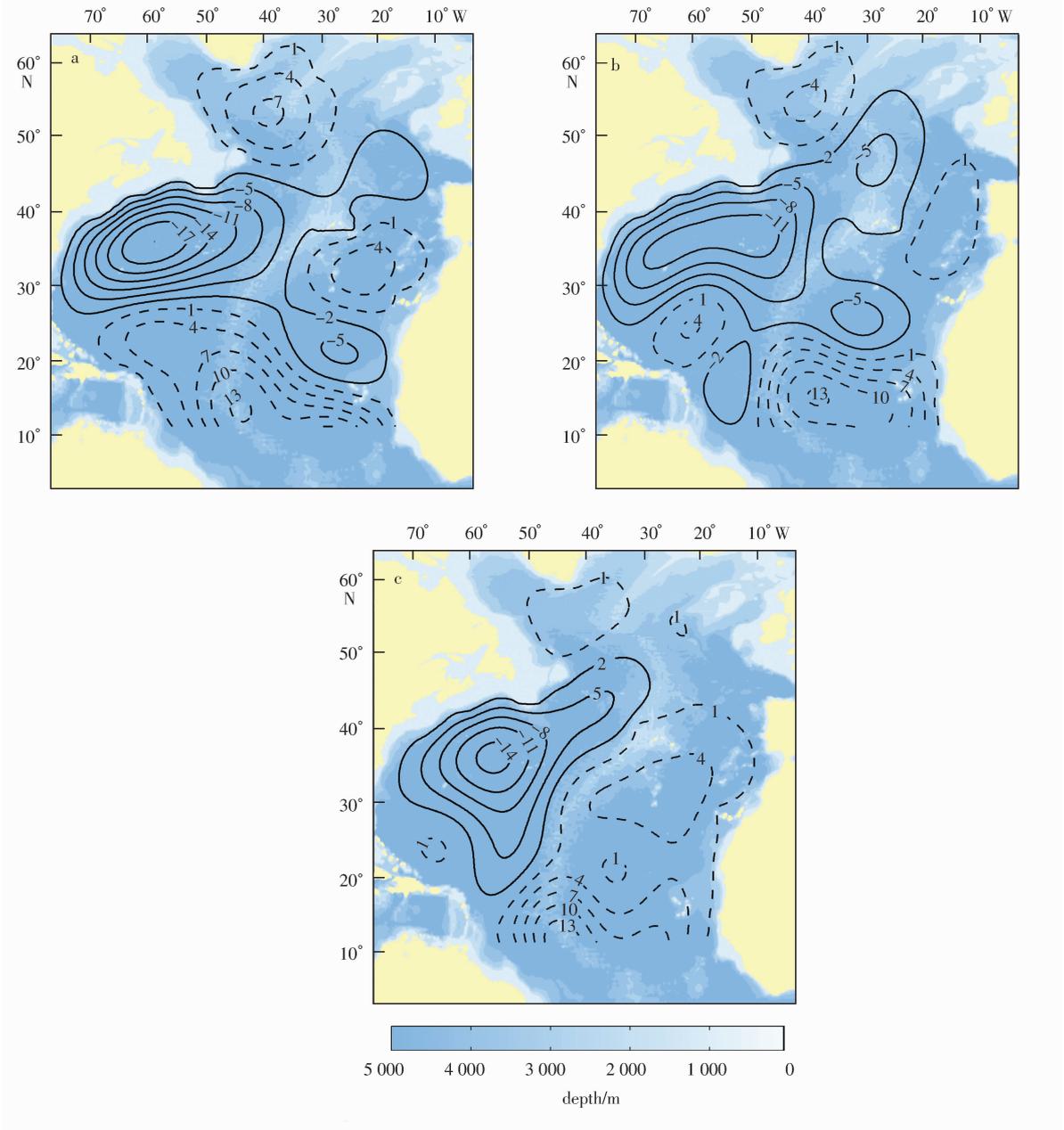

Fig. 4.　Mean stream-function at 1000 m for December 2003—March 2004 (a) April 2004—July 2004 (b) and August 2004 November 2004 (c) computed by the OSD method. Contours are labeled in units of 10^7 cm²/s. The kinematic boundary and open boundary conditions used at Γ_1 and Γ_2, and Γ_3, respectively, are explained in Chu et al. (2003).

The anticyclonic gyre has an intensive core in the western part of the North Atlantic with two branches stretched to the northeastern and southeastern Atlantic (Fig. 4a). The center of the core is not fixed in the same location. It may shift to the northeast by up to 1000 km. The maximum velocity is about 4 ~ 5 cm/s in the core and 0.5 ~ 1 cm/s in the branches of the gyre. The cyclonic gyre stretches from the southeast to northwest up to 25°N with a velocity about 1 ~ 2 cm/s.

The second mode represents a pair of cyclonic and anticyclonic gyres on basin scales (Fig. 4c). However, in this case the cyclonic gyre stretches from the southwest to the northeast up to 43°N and the boundary between these gyres lies along the Mid – Atlantic Ridge. The velocity reaches 3 ~ 4 cm/s in the anticyclonic gyre and 2 ~ 3 cm/s in the cyclonic gyre.

Reid (1994) identified the second mode as the steady state of the North Atlantic due to its high recurrence in data. Our computations indicate that this mode is one of the two possible North Atlantic modes. The two modes correspond to opposite mean values of the North Atlantic oscillation (NAO) index (www. cru. uea. ac. uk): negative value (-0.81) for the first mode (December 2003 to March 2004) and positive value (0.27) for the second (August—November 2004). Explicit and fast transitional inter – mode is clearly seen between April 2004 and July 2004 (Fig. 4b).

It is noted that a cold center is identified near 20°N, 55°W in February 2004 (Fig. 2a) with large spatial gaps in Argo data. Comparing with the reconstructed stream-function from the position data for December 2003—March 2004 (Fig. 4a), a cyclonic circulation is associated with the cold center. This confirms that the southwestern cold center shown in Fig. 2a is physical and not caused by the large spatial gaps in Argo float temperature data. Here, the four months' positioning data (December 2003—

March 2004) is used due to the data sparseness. This also reflects the usefulness of the OSD method.

6   Sensitivity

Our estimations demonstrate that neglecting the vertical shear between 1000 and 1500 m does not cause large bias of the reconstructed circulation patterns (Figs 4 a, b and c). To confirm this, we reconstructed circulation at 1000 m or 1500 m separately in certain regions with the floats parking at the same depth, and compared the circulation patterns in that part of the North Atlantic where these areas intersect. We did not find considerable differences between the circulation patterns at basin – scales.

Mode truncations at 24 for velocity and 38 for temperature are robust to variations of the length of samples (number of observations) and the level of noise distorting the Argo observations. The Euclidean norms $\| A \|_{24}^{2}$ and $\| D \|_{48}^{2}$ increase only for 5% ~ 6% and 1% ~ 3% with the increase of (N, L) to (50, 100), and vary little even if approximately 10% ~ 15% of the data are excluded from the reconstruction process. Robustness of the reconstructed fields is an additional evidence for the reconstruction reliability.

7   Computation error

Velocities computed along original Argo float trajectories (non – filtered) are distorted by quasi – isotropic non – Gaussian white noise with zero mean, standard deviation (5.312 cm/s), skewness (0.034), and kurtosis (6.34), mixed with spatially correlated (red) noise with zero mean, standard deviation (0.049 cm/s), and the correlation radius (150 ~ 200 km). The white noise represents the residual between the original observations and the same observations averaged over 4° × 4° bins. The red noise is the observational velocity minus the sum-

mation of the reconstructed velocities and white noise. Temperature observations are distorted by quasi − Gaussian white noise with zero mean and standard deviation of 0.1 ℃.

The "noise" in the velocity observations can be effectively filtrated by the OSD methad using the rotation method (Chu et al., 2004) if the number of observations is greater than 1800. This requirement can be reached when four months data are used. Similarly, the "noise" in the temperature field can be filtered out if the number of observations is greater than 400. It is possible to use the data within only one month time period.

Our estimations also show that the OSD methad reduces the noise to signal ratio for the Argo data to 0.25 ~ 0.30 (velocity) and 0.07 ~ 0.1 (temperature). With these noise levels, the reconstructed circulation and temperature fields are quite realistic (Chu et al., 2003; Chu et al., 2004).

Errors in estimating the stream-function and temperature are computed using the technology of "laminar ensemble" (Turchin et al., 1971). The reconstruction error for temperature is less than 5% ~ 7% over the whole North Atlantic. The maximum standard deviations of the error for the stream-function is up to 1.6×10^7 cm^2/s in eastern part of North Atlantic and in an area centered at intersection of 20°N parallel and the Mid − Atlantic Ridge. Comparing this error with values of the reconstructed stream-function of 1.0×10^8 cm^2/s for the first area and 4.0×10^7 cm^2/s for the second area, we can conclude that the reconstructed circulation patterns are statistically significant and difference between the modes is not due to noisiness and sparseness of the data and/or unsatisfactory mathematical analysis.

8   Conclusions

The present study demonstrates the usefulness of the Argo float data for identification of basin and subbasin-scale mid-depth circulation in the North Atlantic. The velocity field is quite noisy and sparse when the bin technology is used (see Figs 1a and b). Two different circulation modes and fast transition between them are identified using the optimal spectral decomposition method. The second mode was detected by Reid (1994, see Fig. 8e from his paper) using the climate data arrays. This paper demonstrates that the North Atlantic circulation can switch between two modes rather than "this large − scale pattern of mid − depth flows does not vary too widely" (Reid, 1994). The transition time between the modes is less than three months and there is no seasonal periodicity in temporal mode variability.

References

Argo Science Team. 2001. Argo: the global array of profiling floats. In: Koblinsky C J, Smith N R, eds. Observing the Oceans in the 21st Century. GODAE Project Office, Bureau of Meteorology, Melbourne, 248 ~ 258

Bower A S, Le Cann B, Rossby T, et al. 2002. Directly measured mid-depth circulation in the northeastern North Atlantic Ocean. Nature, 419: 603 ~ 607

Chu P C, Ivanov L M, Margolina T M, et al. 2003a. Analysis of sparse and noisy ocean current data using flow decomposition: Part 1. Theory. J Atmos Oceanic Technol, 20: 478 ~ 491

Chu P C, Ivanov L M, Margolina T M, et al. 2003b. Analysis of sparse and noisy ocean current data using flow decomposition: Part 2. Application to Eulerian and Lagrangian data. J Atmos Oceanic Technol, 20: 492 ~ 512

Chu P C, Ivanov L M, Margolina T M. 2004. Rotation method for reconstructing process and fields from imperfect data. Int J Bifur and Chaos, 14(8): 2991 ~ 2997

Chu P C, Ivanov L M, Melnichenko O V, et al. 2007. On long baroclinic Rossby waves in the tropical North Atlantic observed from profiling floats. J Geophys Res, 112: C05032, doi:10. 1029/2006JC003698

Davis R E. 1991. Observing the general circulation with floats. Deep-Sea Res, 38 (Suppl 1):531 ~ 571

Eremeev V N., Ivanov L M, Kirwan A D, Jr. 1992. Reconstruction of oceanic flow characteristics from quasi − Lagrangian data. J Geophys Res, 97(C6): 9731 ~ 9743

Ichikawa Y, Takatsuki Y, Mizuno K, et al. 2001. Estimation of drifting velocity and error at parking depths for the Argo float. Argo Tech Rep FY2001. Japan Agency for Marine − Earth Science and Technology: 68 ~ 77

Lavender K L, Davis R E, Owens W B. 2000. Direct velocity measurements described a new circulation regime in the Labrador and Irminger Seas, Nature, 407: 66 ~ 69

Lavenberg K L, Owens B, Davis R E. 2005. Mid − depth circulation of the subpolar North Atlantic as measured by surface floats. Deep − Sea Res(I), 52:767 ~ 785

Lozier M S, Owens W B, Curry R G. 1995. The climatology of the North Atlantic. Prog Oceanogr, 36:1 ~ 44

Ivanov L M, Kirwan A D, Jr, Margolina T M. 2001. Filtering noise from oceanographic data with some applications for the Kara and Black Seas, J Mar Sys, 28(1 ~ 2): 113 ~ 139

Paillet J, Archan M, McCartney M S. 1998. Spreading of Labrador Sea water in the eastern North Atlantic, J Geophys Res, 103:10223 ~ 10239

Park J J, Kim K, King B A, et al. 2005. An advanced method to estimate deep currents from profiling floats, J Atmos Oceanic Technol, 22: 1294 ~ 1304

Reid, J L. 1994. On the total geostrophic circulation of the North Atlantic Ocean: flow patterns, tracers, and transports. Prog. Oceanogr, 33:1 ~ 92

Schmitz W J, McCarthey M S. 1993. On the North Atlantic circulation. Rev. Geophys, 31:29 ~ 49

Thiebaux H J, Pedder M A. 1987. Spatial Objective Analysis: with Applications in Atmospheric Science. New York: Academic Press, 299

Turchin V F, Kozlov V P, Malkevich M S. 1971. The use of mathematical − statistics methods for the solution of ill − posed problems. Sov Phys Uspekhi, 103 (3 ~ 4): 681 ~ 703

Vapnik V N. 1982. Estimation of Dependencies based on Empirical Data. New York: Springer − Verlag, 503

Xie J − P, Zhu J, Xu L, et al. 2005. Evaluation of mid − depth currents of NCEP reanalysis data in the tropical Pacific using Argo float position information. Adv Atmos Sci, 22 (5): 677 ~ 684

Zhang H, Prater M D, Rossby T. 2001. Isopycnal Lagrangian statistics from the North Atlantic current RAFOS float observations. J Geophys Res, 106 (C7):13,817 ~ 13,826